

Nuclear shell effect and collinear tripartition of nuclei

A.K. Nasirov^{1,2}, W. von Oertzen³, R.B. Tashkhodjaev²

¹*Joint Institute for Nuclear Research,*

Joliot-Curie 6, 141980 Dubna, Russia,

²*Institute of Nuclear Physics, Uzbek Academy of Science, 100214 Tashkent, Uzbekistan*

³*Helmholtz-Zentrum Berlin, Glienickerstr. 100, 14109 Berlin, Germany*

⁴*Fachbereich Physik, Freie Universität, Berlin*

A possibility of formation of the three reaction products having comparable masses at the spontaneous fission of ^{252}Cf is theoretically explored. This work is aimed to study the mechanism leading to observation of the reaction products with masses $M_1 = 136\text{--}140$ and $M_2 = 68\text{--}72$ in coincidence by the FOBOS group in JINR. The same type of ternary fission decay has been observed in the reaction $^{235}\text{U}(\text{n}_{\text{th}}, \text{fff})$. The potential energy surface for the ternary system forming a collinear nuclear chain is calculated for the wide range of mass and charge numbers of constituent nuclei. The results of the PES for the tri-partition of $^{252}\text{Cf}(\text{sf}, \text{fff})$ shows, that we have favorable dynamical conditions for the formation of fragments with mass combinations of clusters $^{68\text{--}70}\text{Ni}$ with $^{130\text{--}132}\text{Sn}$ and with missing cluster $^{48\text{--}52}\text{Ca}$.

PACS numbers: 21.60.Gx Cluster models; 25.85.Ca Spontaneous fission

I. INTRODUCTION

Binary fission has been studied intensively over the last four decades, for an overview there are the books edited by R. Vandenbosch and J. R. Huizenga [1], C. Wagemans [2], covering all important aspects of this process. A more recent theoretical coverage is available as a textbook by H. Krappe and K. Pomorski in ref. [3]. Ternary fission, when a third light particle is emitted perpendicular to the binary fission axis, has also been studied extensively [4, 5]. The name “ternary” fission has been used so far for such decays by emission of light charged particles with mass numbers ($M < 38$). These ternary decays give decreasing yields as function of increasing mass(charge) of the third particle [4]. The probability of the ternary fission by emission of the alpha particle relative to the binary fission is about $2 \cdot 10^{-3}$ for the

reactions ranging from $^{229}\text{Th}(\text{n}_{\text{th}},\text{f})$ up to $^{251}\text{Cf}(\text{n}_{\text{th}},\text{f})$ [5].

Recent experimental observations of the two fragment yields in coincidences by the two FOBOS-detectors [6, 7] placed at 180° , using the missing mass approach, have established the phenomenon of *collinear cluster tripartition* (CCT) of the massive nuclei. This new decay mode has been observed for the spontaneous decay of $^{252}\text{Cf}(\text{sf},\text{fff})$ and for neutron induced fission in $^{235}\text{U}(\text{n}_{\text{th}},\text{fff})$, see refs. [6–8]. In this CCT with the emission of three fragments, the outer fragments of the “chain” are registered [6] only. The mass number of the missed third fragment can be larger than one of the heaviest light charged particle of the ternary fission above mentioned. Therefore, the CCT process is called as one of the mechanisms of the true ternary fission, when the masses of its products are relatively comparable. The mass correlation plots $M_1 - M_2$ (M_1 and M_2 are mass numbers of products) of the registered reaction products showed the appreciable yield of magic isotopes of $^{68,70}\text{Ni}$, $^{80,82}\text{Ge}$, ^{94}Kr , $^{128,132}\text{Sn}$ and ^{144}Ba . These products were registered in the coincidence, but sum of their mass numbers differs from the total mass numbers M_{CN} of ^{252}Cf and ^{236}U : $M_3 = M_{\text{CN}} - (M_1 + M_2)$, $4 < M_3 < 52$. M_3 is the mass number of the missed fragment at registration. It should be noted that the exotic fission products with mass numbers $61 < M < 76$ (isotopes of Fe, Ni, Zn, Ge) have been observed as the very asymmetric fission products [9–12]. Authors of Ref. [12] concluded that large deformation ($\beta_2=0.84$) of the heavy fragment ^{167}Gd conjugate to ^{70}Ni and transition through a potential barrier with the wide width ($\Delta r=4.5$ fm) can explain the observed unusual small value of the kinetic energy of the light fission product of $^{236}\text{U}(\text{n},\text{f})$ reaction ($E_{\text{n}}=1$ MeV). The aim of the present work is to analyze the formation of the $^{68,70}\text{Ni}$ clusters in the true ternary fission of ^{252}Cf and $^{235}\text{U}(\text{n}_{\text{th}},\text{f})$.

II. TRUE TERNARY FISSION

The above mentioned experimental observations of the two fragment yields in coincidences by the two FOBOS-detectors [6, 7] placed at 180° have given an evidence of the true ternary fission, which was predicted in the theoretical works [13–16] for long time ago. The collinear configuration is preferred relative to the oblate configuration for heavy system of ternary fragments with larger charges and masses [16]. In the last paper, the results of potential energy and relative yield calculations reveal that collinear configuration increases the probability of emission of heavy fragments like ^{48}Ca and its neighboring nuclei as the

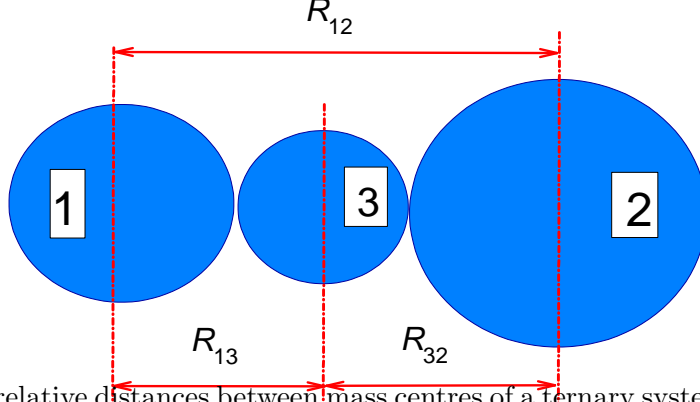


FIG. 1. The relative distances between mass centres of a ternary system for collinear configuration.

third fragment. The latter, Ca, as the smallest third particle is positioned along the line connecting Sn and Ni, in this way minimizing the potential energy. In the experiments described in Refs. [6, 7], two of the three fragments moving in the opposite directions were detected. The third fragment could not be registered due to the smallness of its velocity. The range of the kinetic energy values was studied in Ref. [17]. Thus binary coincidences of the $^{68,70}\text{Ni}$ isotopes and fission products with $A \approx 132$ are observed in the spontaneous fission of ^{252}Cf and $^{235}\text{U}(\text{n}_{\text{th}}, \text{f})$ reaction [6, 7]. At the observation of $^{68,70}\text{Ni}$ in the former and latter reactions the missed fragments are Ca and Si isotopes, respectively. To study theoretically the possibility of the formation of $^{68,70}\text{Ni}$ isotopes in coincidence with the fission product having the mass number $A \approx 132$ — 136 , in the present work, the potential energy surface (PES) of the ternary system is calculated and analyzed.

A. Potential energy surface for the ternary system

PES is found as a sum of the energy balance of the interacting fragments and nucleus-nucleus interaction between them

$$U(R_{13}, R_{23}, Z_1, Z_3, A_1, A_3) = Q_{\text{ggg}} + V_{12}^{(\text{Coul})}(Z_1, Z_2, R_{13} + R_{23}) + V_{13}(R_{13}, Z_1, Z_3, A_1, A_3) + V_{23}(R_{23}, Z_3, Z_2, A_3, A_2), \quad (1)$$

where $Q_{\text{ggg}} = B_1 + B_2 + B_3 - B_{\text{CN}}$ is the balance of the fragments binding energy at the ternary fission; the values of binding energies are obtained from the mass table in Ref. [18]; V_{13} and V_{23} are the nucleus-nucleus interaction of the middle cluster “3” (A_3 and Z_3 are its mass and charge numbers, respectively) with the left “1” (A_1 and Z_1) and right “2” (A_2 and Z_2) fragments of the ternary system; $V_{12}^{(\text{Coul})}$ is the Coulomb interaction between two border

fragments “1” and “2”, which are separated by the distance $R_{13} + R_{23}$, where R_{13} and R_{23} are the distances between the middle cluster and two outer clusters placed on the left and right sides, respectively (see Fig. 1). The interaction potentials V_{13} and V_{23} consist of the Coulomb and nuclear parts:

$$V_{3i}(R_{3i}, Z_i, Z_3, A_i, A_3) = V_{3i}^{(\text{Coul})}(Z_i, Z_3, R_{i3}) + V_{3i}^{(\text{Nucl})}(Z_i, A_i, Z_3, A_3, R_{3i}), \quad \text{where } i = 1, 2. \quad (2)$$

The nuclear interaction calculated by the double folding procedure with the effective nucleon-nucleon forces depending on nucleon distribution density (see Ref. [19]). The Coulomb interaction is determined by the Wong formula [20].

Theoretical interpretation of the collinear tri-partition of ^{252}Cf and ^{236}U [6–8] needs the knowledge about the mechanism of fission of the residual super-deformed system. The sequential mechanism of the true ternary fission without correlation between two ruptures of the two necks connecting three fragments in collinear configuration was assumed in Ref. [19]. The realization of the asymmetric fission channel as the first stage of sequential mechanism was considered. At the second stage the heavy product undergoes fission forming two nuclei with comparable masses. The probability of fission depends on the fission barrier, which is very high for the relatively light nuclei. For example, the fission probability of the nuclei lighter than ^{158}Ce formed with large probability at fission of actinides is very small (see Table 1 and Ref. [19]). To estimate the yield of the ternary fission products in different channels, we compared the yield of the reaction products in fission of ^{144}Ba , ^{150}Ce and ^{154}Nd **Table 1**. The realization probabilities of the different sequential channels for the collinear cluster tripartition of $^{236}\text{U}^*$. “*” means that these nuclei are excited.

Fission channel	Fission channel of	Probability
$^{236}\text{U}^* \rightarrow f_1 + f_2$	primary heavy fragment	of CCT
$^{82}\text{Ge}^* + ^{154}\text{Nd}^*$	$^{154}\text{Nd}^* \rightarrow ^{72}\text{Ni}^* + ^{82}\text{Ge}^*$	$3 \cdot 10^{-4}$
	$^{154}\text{Nd}^* \rightarrow ^{76}\text{Zn}^* + ^{78}\text{Zn}^*$	$1.5 \cdot 10^{-4}$
$^{86}\text{Se}^* + ^{150}\text{Ce}^*$	$^{150}\text{Ce}^* \rightarrow ^{66}\text{Fe}^* + ^{82}\text{Ge}^*$	$1.0 \cdot 10^{-5}$
	$^{150}\text{Ce}^* \rightarrow ^{72}\text{Ni}^* + ^{76}\text{Zn}^*$	$1.4 \cdot 10^{-5}$

[19], which are formed in the primary fission of ^{236}U (see Fig. 2).

The yield of fission products is calculated using the statistical method based on the driving potentials for the fissionable system (see Ref. [19]). The minima of the potential

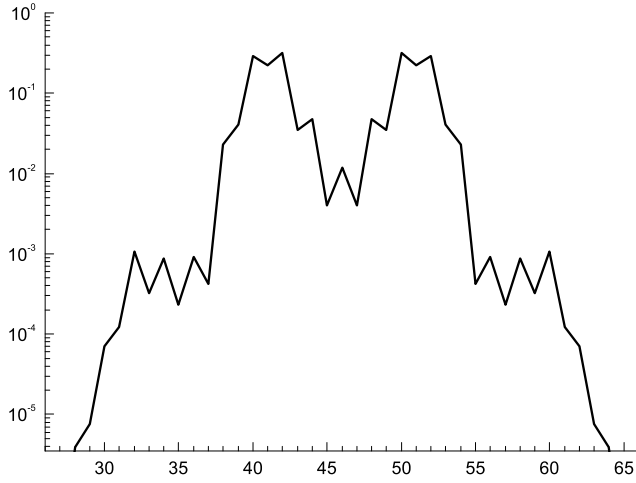


FIG. 2. Yields of the reaction products at the binary fission of ^{236}U calculated with the statistical method as in Ref. [19].

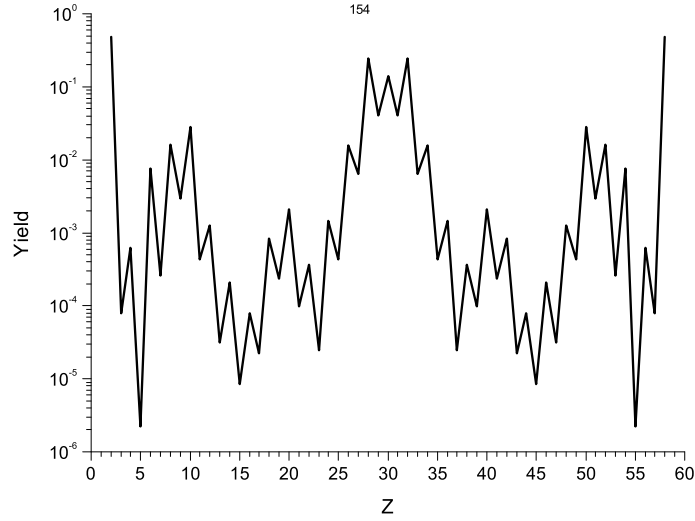


FIG. 3. Yields of the reaction products at the (sequential) fission of ^{154}Nd formed in the first step at binary fission of ^{236}U .

energy of the decaying system correspond to the charge numbers of the products, which are produced with large probabilities in the sequential fission of the mother nucleus.

The probability of the yield of the ternary fission products is relatively large in the case of splitting of ^{154}Nd as the second step of sequential fission. The results for the yield of the ^{154}Nd products are presented in Fig. 3. Comparison of the theoretical results for the yield of the true ternary fission products (open squares and diamonds) with the observed yields of corresponding mass-mass distribution is presented in Fig. 4. The experimental data (filled up and down triangles) presented in Fig. 4 are the mass-mass distribution of the $^{235}\text{U}(n_{\text{th}}, f)$ fission fragments registered in coincidence by two detectors opposite relative to

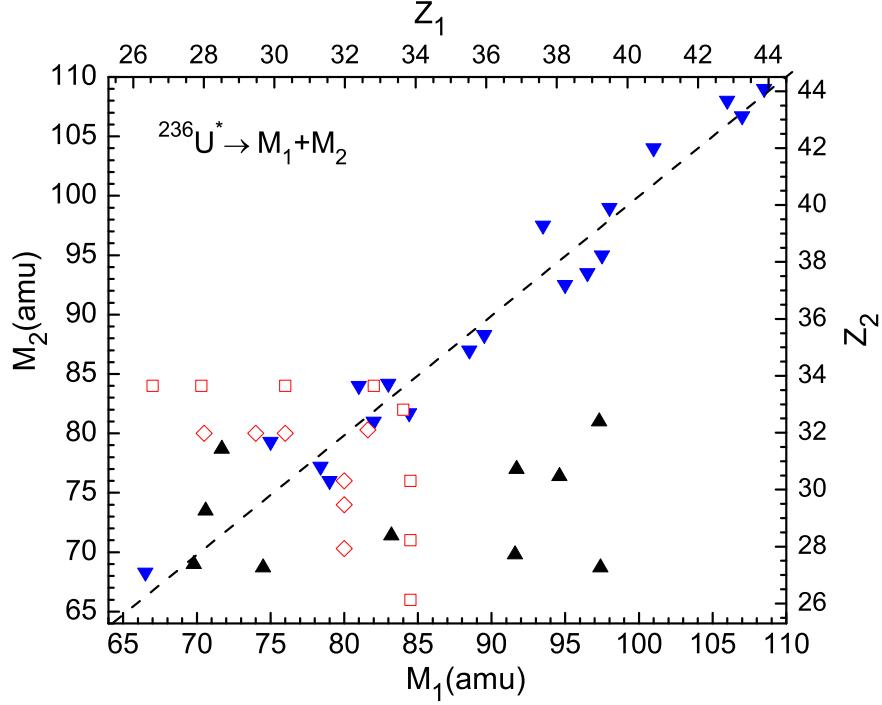


FIG. 4. Comparison of the maximum values of the calculated yield of the collinear cluster tripartition products in the sequential fission $^{82}\text{Ge} + (^{154}\text{Nd} \rightarrow \{^{72}\text{Ni} + ^{82}\text{Ge}, ^{76}\text{Zn} + ^{78}\text{Zn}\})$ (diamonds) and $^{86}\text{Se} + (^{150}\text{Ce} \rightarrow \{^{68}\text{Fe} + ^{82}\text{Ge}, ^{72}\text{Ni} + ^{78}\text{Zn}\})$ (squares) mechanisms with the experimental data of the mass-mass distribution of the CCT products in the $^{235}\text{U}(n_{\text{th}}, f)$ reaction: with the ones registered in coincidence with approximately equal momenta (up triangles, the data were taken from Figure 6b of ref. [21]) and with the ones having approximately equal masses with the momentum values up to $120 \text{ amu}(\text{cm ns})^{-1}$ (down triangles, the data from Figure 7d of ref.[21]). The charge numbers corresponding to the presented mass numbers are shown on the top and upper axes.

the ^{235}U target. Different filled symbols correspond to the CCT events, which are selected from the whole data by different conditions: 1) the CCT products with approximately equal momenta, velocities (filled up triangles, the results were taken from Fig. 6b of ref. [21]) and 2) the CCT products with approximately equal masses with the momentum values up to $120 \text{ amu}(\text{cm ns})^{-1}$. The results of Ref. [19] could interpret only the yield of the true ternary fission products with comparable masses. The probability of the yield of the CCT products in the sequential fission channels of ^{236}U , which start with the $^{82}\text{Ge}^* + ^{154}\text{Nd}^*$ and $^{86}\text{Se}^* + ^{150}\text{Ce}^*$ channels are compared in Table 1. From the Table 1 is seen that production of the Ni isotope is more probable in the fission of ^{154}Nd .

But these events do not correspond to the dominant processes where the 10^{-3} yields of

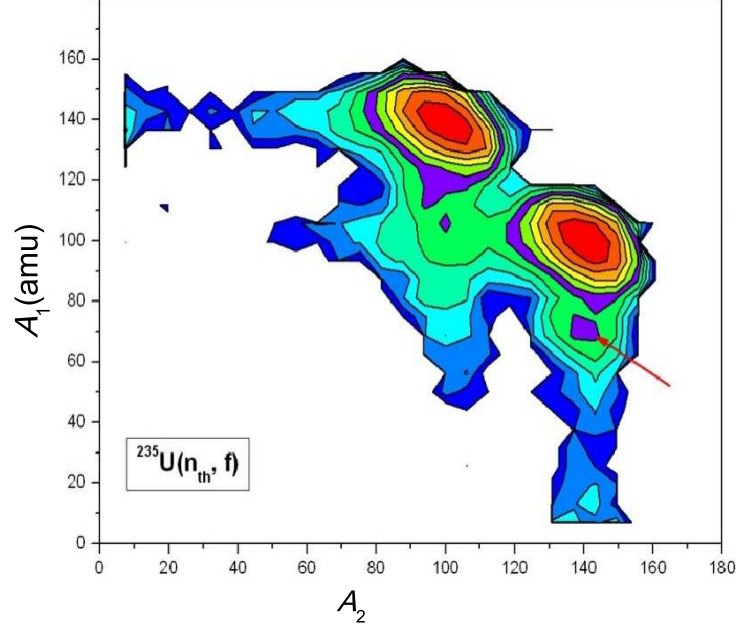


FIG. 5. Contour map of the mass-mass distribution (logarithmic scale, with lines approximately a step factor of 1.5) from a coincidence in the two opposite detectors. The bump in the spectrometer arm1 facing the backing of the U source is marked by the arrow (from Ref. [6]).

$^{68-70}\text{Ni}$ per binary fission were observed [6, 7] with relatively large probability in coincidence with the products with masses $A = 130-150$ in the $^{235}\text{U}(n_{\text{th}}, f)$ (see Fig. 5) reaction.

III. ABOUT RELATION BETWEEN THE TWO STEPS OF THE SEQUENTIAL FISSION

The role of the nuclear shell structure is important in the formation of the ternary system of nuclei and some of them should have magic or near magic numbers for neutrons or/and protons. This is a necessary condition for the realization of the true ternary fission as one channel of the spontaneous fission of ^{252}Cf . But the existence of the ternary system as the intermediate state of a system undergoing to fission is not enough for the occurrence of the true ternary fission. Three products can be observed, when the other massive super-deformed (residual) part undergoes to fission forming the two other products. The mechanism of sequential ternary fission with the short time between ruptures of two necks connecting the middle cluster 3 to the outer nuclei 1 and 2 may be responsible for the formation of the observed CCT products in Refs. [6, 7]. As we stressed above the reason for smallness of the fission probability of the light strongly deformed fragment, which is formed after separation

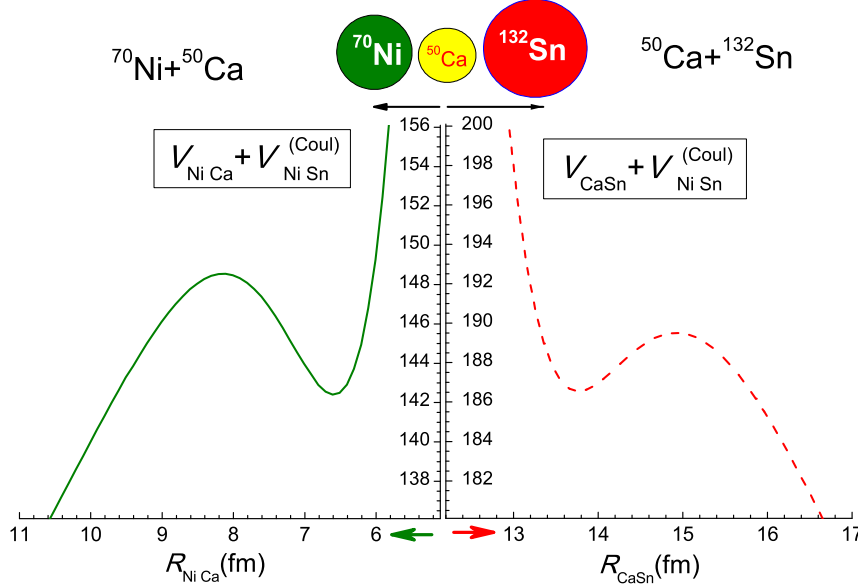


FIG. 6. The nucleus-nucleus interactions between $^{70}\text{Ni}+^{50}\text{Ca}$ (left part) and $^{50}\text{Ca}+^{132}\text{Sn}$ (right part) of the ternary system as a function of the relative distances between their mass centres for the collinear configuration.

of the tin-like nucleus, is its large fission barrier ($B_f > 20$ MeV). Our calculations showed that the value of B_f decreases if the heavy tin-like nucleus is not far from the other residual part of fission: after the first rupture, its Coulomb field makes a smaller potential well in the interaction potential between the formed fragments at fission of the light super-deformed nucleus. In the case of spontaneous fission of ^{252}Cf , this super-deformed nucleus is ^{120}Cd , which can be considered as a dinuclear system consisting of ^{70}Ni and ^{50}Ca .

The depth of the potential well for the massive system ($\text{Ca}+\text{Sn}$) is smaller than for the one for the light system ($\text{Ca}+\text{Ni}$). In the case of the asymmetric system the decay probability for the heavy fragment is larger since the depth of the potential well is smaller due to larger Coulomb repulsion from the middle cluster: $Z_1 \cdot Z_3 < Z_2 \cdot Z_3$ if $Z_1 < Z_2$. It is seen from Fig. 6, which is calculated for the configuration $^{70}\text{Ni}+^{50}\text{Ca}+^{132}\text{Sn}$. Therefore, ^{132}Sn , or the product close to ^{132}Sn , is separated as the first product of the fission process. According to the mechanism assumed in our calculations the rupture of the second neck occurs while the first product is just being accelerated and not far from the dinuclear system consisting of $^{70}\text{Ni}+^{50}\text{Ca}$. This is seen from the contour plot in Fig. 7, where the dependence of the total interaction potential V_{int} of the collinear ternary system $^{70}\text{Ni}+^{50}\text{Ca}+^{132}\text{Sn}$ is presented as a

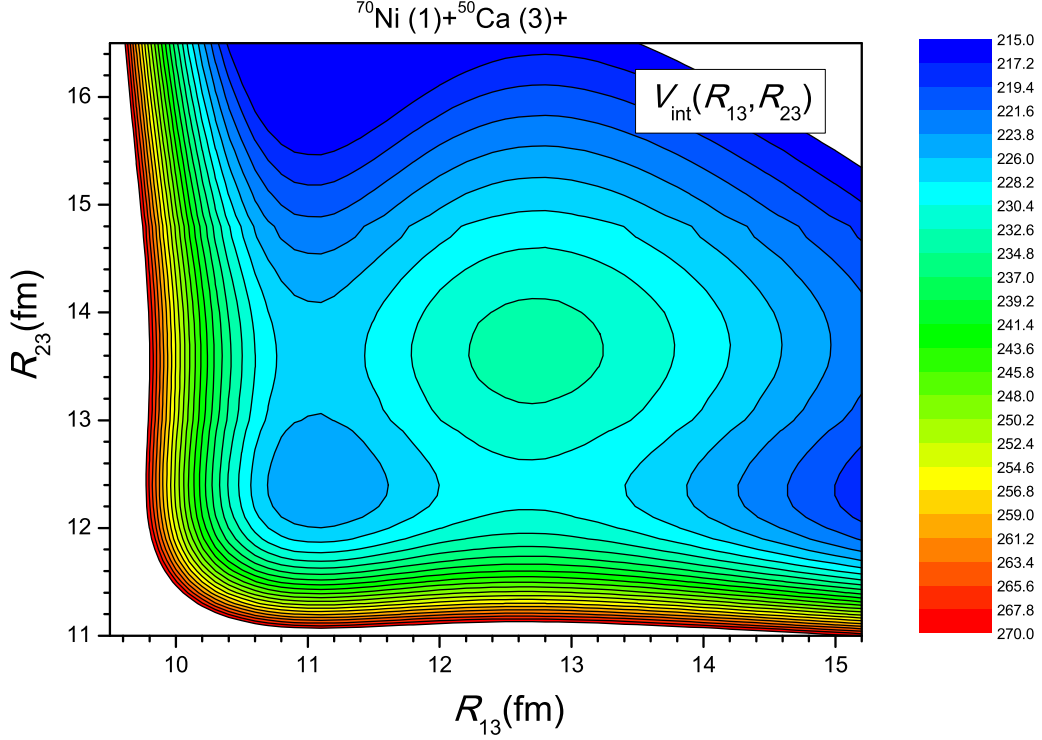


FIG. 7. The contour plot of the total interaction potential V_{int} of the collinear ternary system $^{70}\text{Ni} + ^{50}\text{Ca} + ^{132}\text{Sn}$ as function of the relative distances R_{13} and R_{23} between the centre of the middle cluster and outer nuclei. $V_{\text{int}} = \sum_{i=1,2} V_{3i}(R_{3i}, Z_i, Z_3, A_i, A_3) + V_{12}^{(\text{Coul})}(Z_1, Z_2, R_{12})$

function of the relative distances R_{13} and R_{23} between centres of the middle cluster and outer nuclei. This potential includes the Coulomb potential $V_{12}^{(\text{Coul})}(Z_1, Z_2, R_{12})$ between the border nuclei “1” and “2” in addition to the sum of the Coulomb and nuclear interaction between neighbor nuclei (“13” and “32”). The minimum of the potential well corresponds to the equilibrium state of the system. The barrier of the potential in the direction of the relative distance “ R_{23} ” is lower than the barrier in the direction “ R_{13} ”. The interaction potentials between neighbor fragments at the fixed distance between the middle and other fragment are shown in Fig. 7. Therefore, due to excitation energy of vibration degrees of freedom the massive fragment, *i.e.* Sn, separates first. But the penetration through the barrier R_{13} is possible while the separated Sn nucleus is not far from the system $^{70}\text{Ni} + ^{50}\text{Ca}$. The realization of this mechanism can explain the observation of the true ternary fission as the yield of Ni isotopes in coincidence with the massive product $A \approx 140$ in the experiments of the FOBOS-group [6, 7]. The distances R_{13} and R_{23} between interacting nuclei corresponds to the minimum values of the potential wells of V_{13} and V_{23} interactions, respectively, which are affected by the Coulomb interaction $V_{12}^{(\text{Coul})}$ of the border fragments (see Fig. 6).

The procedure of the PES calculation is organized as following. For the given values of charge Z_3 and mass A_3 numbers of the fragment “3” the values of U (PES) are calculated by varying Z_1 from 2 up to 52 and A_1 in the wide range providing the minimum value of U at the fixed Z_1 and Z_3 (A_3). The same procedure is made for the range of A_3 values at each mass and charge configuration of a ternary system. The interaction potentials $V_{13}+V_{12}^{(\text{Coul})}$ and $V_{23}+V_{12}^{(\text{Coul})}$ for the ternary system $^{70}\text{Ni}+^{50}\text{Ca}+^{132}\text{Sn}$ are presented on the left and right part of Fig. 6. The pre-scission state of the ternary system is determined by the minimum values of the potential wells in the interaction potentials $V_{ik}(R_{ik})$ in expression for PES Eqn. (1).

The probability of this configuration is large according to the landscape of PES calculated for the ternary system of ^{252}Cf . The contour plot of PES for the ternary system formed at the spontaneous fission of ^{252}Cf is presented in Fig. 8 as a function of the charge and mass numbers of fragments “1” and “3”. The decay is considered with two sequential neck ruptures [22]. The rupture of the necks means overcoming or tunneling through the barriers, which are illustrated in Fig. 6. It should be noted that the middle cluster is formed as neutron richer in comparison with the border fragments. The reason of this theoretical phenomenon is connected with the use of the effective nucleon-nucleon forces suggested by Migdal [23], which depend on isospin in calculations of the nuclear part of the nucleus-nucleus interaction. From the minimizing procedure of the PES by the distribution of neutrons between fragments Z_1, Z_2 , and Z_3 we found that the pre-scission configuration $^{70}\text{Ni}+^{50}\text{Ca}+^{132}\text{Sn}$ has lower potential energy in comparison with those containing the other isotopes ($A \neq 50$) of Ca as the middle cluster [24].

This is demonstrated in Fig. 9, where the values of the PES calculated for the configurations of the ternary system with different isotopes of Ca (middle cluster) are compared. In Fig. 9 we represent also the curve of results, which were calculated for the other case, when the middle cluster is Ni: $^{48}\text{Ca}+^{72}\text{Ni}+^{132}\text{S}$. The minimum energy of the last configuration is much higher than the one obtained for the $^{70}\text{Ni}+^{50}\text{Ca}+^{132}\text{Sn}$ case. This means that the population of the configuration with Ni as the middle cluster is much less probable.

Two important conclusions from the attempt of theoretical analysis of the experimental results [6, 7] of the FOBOS-group presented in Fig. 5 are 1) the correct estimation of the ternary system configuration in the pre-scission state and 2) the availability of the external Coulomb field causing sequential fission of the super-deformed light residual mononucleus

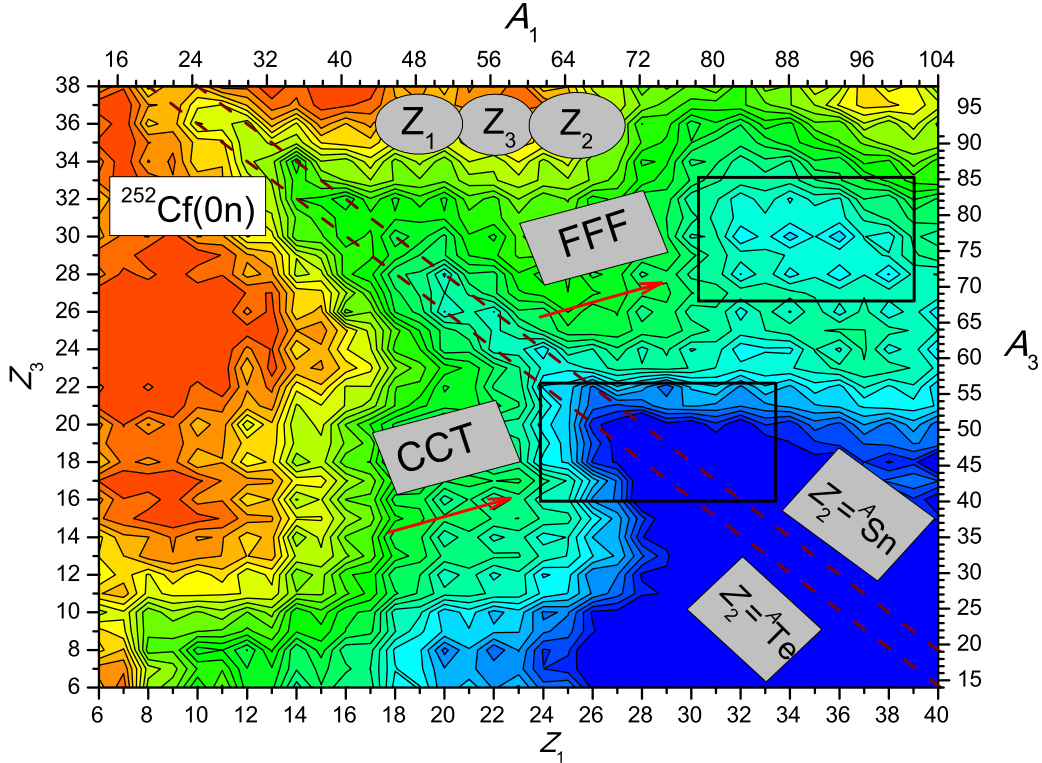


FIG. 8. The contour plots of PES calculated for the ternary decays characterized by fragments Z_1 (A_1) and Z_3 (A_3) for ^{252}Cf . The cases with the formation of the isotopes of Tin and Tellurium, $^{A}_{50}\text{Sn}$ and $^{A}_{52}\text{Te}$, as the fragments with Z_2 are shown by dashed lines. FFF shows the area of the formation of the three fragments with nearly equal masses.

accompanying formation of the fragments $A = 130$ — 150 in the first step.

IV. CONCLUSION

Results of the PES for the ternary fission of ^{252}Cf are presented as a binary correlation function of the charge and mass numbers of the middle cluster (Z_3, A_3) and one of the outer fragments (Z_1, A_1). There are valleys on the PES corresponding to the formation of the cluster $Z_2 = ^{132}\text{Sn}$ at the different values of Z_1 and Z_3 . This landscape of PES is related to the long tail in the mass-mass distributions of the experimentally registered products M_1 and M_2 demonstrating the persistence of shell structure in the double magic nucleus ^{132}Sn . The PES contains local minima showing the favored population of the cluster configurations $^{132}\text{Sn} + ^{50}\text{Ca} + ^{70}\text{Ni}$, $^{132}\text{Sn} + ^{38}\text{S} + ^{82}\text{Ge}$, $^{132}\text{Sn} + ^{36}\text{Si} + ^{84}\text{Se}$, $^{150}\text{Ba} + ^{22}\text{O} + ^{80}\text{Ge}$ and other configurations. We found that the middle cluster is more neutron rich than outer fragments. The experimentally observed yield of $^{68,70}\text{Ni}$ isotopes (see Fig. 5) is related to the

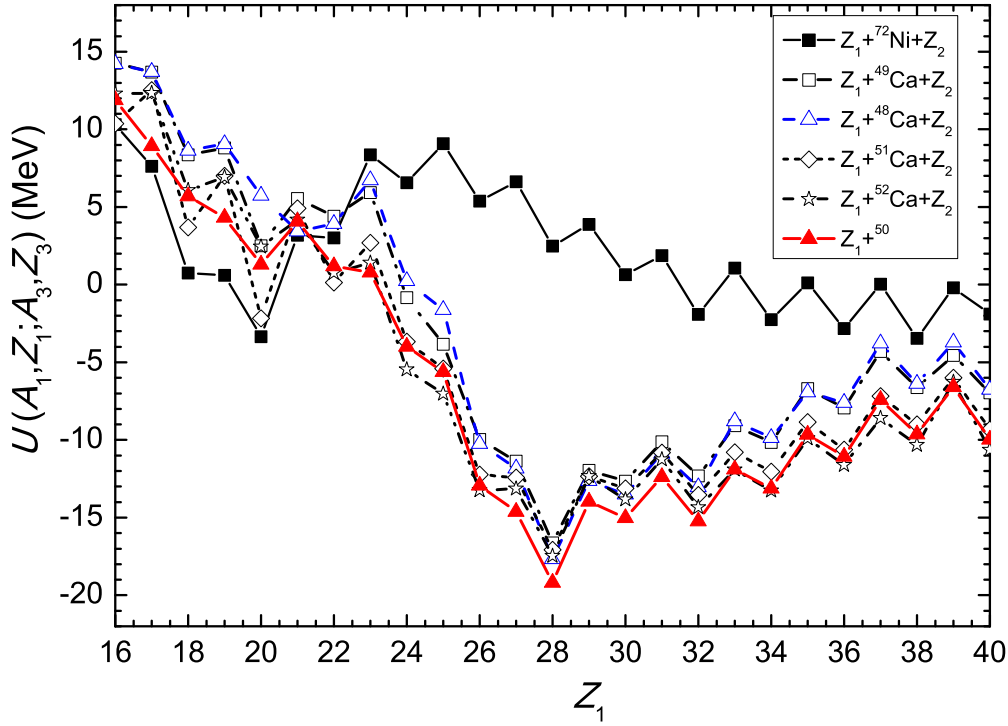


FIG. 9. Comparison of the PES calculated for the pre-scission state of the collinear ternary system $Z_1 + {}^A\text{Ca} + Z_2$ formed in the spontaneous fission of ${}^{252}\text{Cf}$ and for the configuration $Z_1 + {}^{72}\text{Ni} + Z_2$, (black squares) as function of Z_1 .

configuration ${}^{132}\text{Sn} + {}^{50}\text{Ca} + {}^{70}\text{Ni}$ of the ternary system. The rupture of the neck connecting ${}^{132}\text{Sn}$ to the middle cluster takes place earlier than the rupture connecting ${}^{68,70}\text{Ni}$ to the ${}^{50}\text{Ca}$. The position of the minimum energy on PES for the ${}^{132}\text{Sn} + {}^{72}\text{Ni} + {}^{48}\text{Ca}$ is much higher (by 15 MeV) than the one for the configuration ${}^{132}\text{Sn} + {}^{50}\text{Ca} + {}^{70}\text{Ni}$. Therefore, the small population is observed for the configuration with Ni as the middle cluster, and the contribution of this channel is observed to be quite small by the FOBOS-group.

ACKNOWLEDGMENTS

Authors thank Y. Pyatkov and D. Kamanin for their important discussions of true ternary fission mechanism and providing us with the data shown in the Fig. 5. A.K.N. is grateful to Profs. Dipak Biswas for the support and warm hospitality during his staying in India. W.v.O. thanks the FLNR and BLTP of JINR for their hospitality extended to him during his stays in Dubna.

- [2] C. Wagemans, ed. *The nuclear fission process* (CRC Press Inc., 1991)
- [3] H. Krappe and K. Pomorski in *Lecture Notes in Physics* Vol. **838** (Springer-Verlag, Heidelberg, 2012)
- [4] F. Gönnenwein, *Nucl. Phys. A* **734**, 213, (2004).
- [5] F. Gönnenwein, in *Europhysics News* **36/1**, 11 (2005).
- [6] Yu. V. Pyatkov *et al.* *Eur. Phys. J. A.* **45**, 29 (2010).
- [7] Yu. V. Pyatkov *et al.* *Eur. Phys. J. A.* **48**, 94 (2012).
- [8] W. von Oertzen, Y. V. Pyatkov and D. Kamanin, *Acta Phys. Polonica* **44**, 447 (2013).
- [9] V. K. Rao, V. K. Bhargava, S. G. Marathe, S. M. Sahakundu, and R. H. Iyer, *Phys. Rev. C* **19**, 1372 (1979)
- [10] G. Barreau, et al. *Nucl. Phys. A* **432**, 411 (1985).
- [11] J.L. Sida, *Nucl. Phys. A* **502**, 233c (1989)
- [12] A.A. Goverdovsky et al., *Physics of Atomic Nuclei (Yadernaya Fizika)* **58**, 1546 (1995).
- [13] H. Diehl, W. Greiner, *Nucl. Phys. A.* **229**, 29 (1974).
- [14] D. N. Poenaru, R. A. Gherghescu, W. Greiner, *Nucl. Phys. A* **747**, 182 (2005).
- [15] G. Royer, *J. Phys. G: Nucl. Part. Phys.* **21**, 249 (1995).
- [16] K. Manimaran and M. Balasubramaniam, *Phys. Rev. C.* **83**, 034609 (2011).
- [17] K.R. Vijayaraghavan, W. von Oertzen and M. Balasubramaniam, *Eur. Phys. J. A* **48**, 27 (2012).
- [18] G. Audi, A.H. Wapstra and C. Thibault, *Nucl. Phys. A* **729**, 337 (2003).
- [19] R. B. Tashkodajev, A. K. Nasirov and W. Scheid, *Eur. Phys. J. A.* **47**, 136 (2011).
- [20] C. Y. Wong, *Phys. Rev. Lett.* **31**, 766 (1973).
- [21] Yu. V. Pyatkov *et. al.*, *Physics of Atomic Nuclei*, **73**, 1309 (2010)
- [22] W. von Oertzen and A.K. Nasirov, *Phys. Lett. B* **734**, 234 (2014).
- [23] A.B. Migdal, *Theory of the Finite Fermi Systems and Properties of Atomic Nuclei* (Nauka, Moscow, 1983).
- [24] A.K. Nasirov, W. von Oertzen, A.I. Muminov and R B Tashkhodjaev, *Phys. Scr.* **89**, 054022 (2014).